Published in final edited form as:
Neurosurgery. 2015 February ; 76(2): 115–124. doi:10.1227/NEU.0000000000000622.

Fluorescent Cancer-Selective Alkylphosphocholine Analogs For Intraoperative Glioma Detection

Kyle I. Swanson, MD[1], **Paul A. Clark, PhD**[1], **Ray R. Zhang, BS**[1,2], **Irawati K. Kandela, PhD**[6], **Mohammed Farhoud, MS**[3], **Jamey P. Weichert, PhD**[3,4,5,6], and **John S. Kuo, MD PhD**[1,2,5,7]

[1]Dept. of Neurological Surgery, University of Wisconsin School of Medicine and Public Health, Madison, WI, USA

[2]Cell and Molecular Biology Training Program, University of Wisconsin School of Medicine and Public Health, Madison, WI, USA

[3]Dept. of Radiology, University of Wisconsin School of Medicine and Public Health, Madison, WI, USA

[4]Dept. Medical Physics, University of Wisconsin School of Medicine and Public Health, Madison, WI, USA

[5]Carbone Cancer Center, University of Wisconsin School of Medicine and Public Health, Madison, WI, USA

[6]Cellectar Biosciences, Inc., Madison, WI, USA

[7]Dept. of Surgery, National University of Singapore, Singapore

Abstract

Background—5-ALA induced tumor fluorescence aids brain tumor resections but is not approved for routine use in the United States. We developed and describe testing of two novel fluorescent, cancer-selective alkylphosphocholine analogs, CLR1501 (green) and CLR1502 (near-infrared), in a proof-of-principle study for fluorescence-guided glioma surgery.

Objective—To demonstrate CLR1501 and CLR1502 are cancer cell-selective fluorescence agents in glioblastoma models and compare tumor (T) to normal brain (N) fluorescence ratios with 5-ALA.

Methods—CLR1501, CLR1502, 5-ALA were administered to mice with MRI-verified orthotopic U251 GBM and GSC-derived xenografts. Harvested brains were imaged using confocal

Corresponding Author: John S. Kuo, MD PhD FAANS FACS Dept. of Neurological Surgery University of Wisconsin School of Medicine and Public Health Box 8660 Clinical Science Center 600 Highland Ave Madison, WI 53792 j.kuo@neurosurgery.wisc.edu Phone: (608) 262-7303 Fax: (608) 263-1728.

Disclosure: J.P.W. is a cofounder of Cellectar Biosciences Inc., which owns licensing and patent rights to CLR1501, CLR1502 and related agents described in this paper. The other authors have no personal, financial, or institutional interest in any of the drugs, materials, or devices described in this article.

Data and materials availability: CLR analogs and GSC lines can be requested via material transfer agreements from Cellectar Biosciences, Inc. or the University of Wisconsin-Madison, respectively.

A video abstract discussion by Drs. Kuo and Weichert accompanies this article. Scan the QR code to view this video.

Supplemental Digital Content, Video. CLR1502 fluorescence visualization of U251-derived xenograft in mouse.

microscopy (CLR1501), IVIS Spectrum imaging system (CLR1501, CLR1502, and 5-ALA), or Fluobeam near-infrared fluorescence imaging system (CLR1502). Imaging and quantitative analysis of T:N fluorescence ratios were performed.

Results—Excitation/emission peaks are 500/517nm for CLR1501, and 760/778nm for CLR1502. The observed T:N ratio of CLR1502 (9.28±1.08) was significantly higher ($p<0.01$) than CLR1501 (3.51±0.44 on confocal imaging; 7.23±1.63 on IVIS imaging) and 5-ALA (4.81±0.92). Near-infrared Fluobeam CLR1502 imaging in a mouse xenograft model demonstrated high contrast tumor visualization compatible with surgical applications.

Conclusion—CLR1501 (green) and CLR1502 (near infrared) are novel tumor-selective fluorescent agents for discriminating tumor from normal brain. CLR1501 exhibits a tumor to brain fluorescence ratio similar to 5-ALA, whereas CLR1502 has a superior tumor to brain fluorescence ratio. This study demonstrates the potential use of CLR1501 and CLR1502 in fluorescence-guided tumor surgery.

Keywords

glioblastoma; intraoperative imaging; optical imaging; tumor fluorescence

INTRODUCTION

Background

Evidence has accumulated that achieving a radiographic gross total resection (GTR) in high-grade gliomas (HGG) improves overall survival. Two retrospective case-controlled series reported that GTR significantly improved overall survival from 8 months to 13 months.[1,2] Despite evidence for a survival benefit, the overall rate of achieving GTR is relatively low. A literature meta-analysis found that the GTR rate was 62.3% (range of 33-76%) for HGG.[3] Other reports suggest that even when tumor anatomy prevents safe GTR, maximizing extent of resection (EOR) for HGG increases overall survival. Sanai *et al* found a survival benefit even for a subtotal EOR down to 78%.[4] The goal of increasing EOR to reduce tumor burden and improve survival must be balanced against the higher risk of neurological deficits associated with more extensive resections, especially since postoperative neurological deficit is associated with diminished quality of life (QOL) and survival.

Many innovative technologies are being developed to improve tumor visualization and optimize strategies for maximal safe resection.[5] Innovations such as the operative microscope, intraoperative ultrasound, image-guided neuronavigation, and intraoperative MRI have been applied to improve tumor surgery.[6] Fluorescence agents for tumor detection or visualization is a promising new strategy to discriminate tumor from normal tissue, and being studied for maximizing safe surgical resection in multiple cancers, including bladder cancer, ovarian cancer, and brain tumors.[7,8,9]

5-aminolevulinic acid (5-ALA) is currently approved in Europe for fluorescence-guided neurosurgery. 5-ALA is converted in tumors via the porphyrin synthesis pathway to protoporphyrin IX (PpIX, fluorescent excitation peak 405 nm, emission peak 635 nm).[10] Stummer *et al.* demonstrated that oral 5-ALA administration leads to relative accumulation

of fluorescent PpIX in HGG, which discriminates tumor from normal brain in both rodents and humans.[9,11-13] A phase IIIA trial comparing 5-ALA guided HGG resection versus standard microsurgery showed improved GTR (36% versus 65%), and better 6 month progression-free survival (41% versus 21%).[14] Based on the above study, 5-ALA use for HGG resection has been adopted internationally; but since the study was not powered adequately to address overall survival and did not involve US sites, 5-ALA is still not FDA-approved for routine use in America.

5-ALA guided fluorescence of malignant gliomas provides unprecedented high positive predictive value and sensitivity.[15-19] Several methods are also being developed and tested to detect cases of low or variable tumor PpIX fluorescence signal, including intraoperative confocal microscopy[3,20-24] and intraoperative spectroscopy.[25-28] It is also unknown whether 5ALA detects clinically significant subsets of cancer cells such as cancer stem cells. Therefore, many investigators are interested in developing new tumor visualization agents and technologies.

We recently reported preclinical and early human studies of cancer-targeted alkylphosphocholine (APC) analogs based on CLR1404 (18-(p-iodophenyl) octadecylphosphocholine), that display prolonged tumor-selective retention in many different cancers via testing of 55 different *in vivo* rodent and human cancer, and cancer stem cell models.[29] Extensive *in vitro* and *in vivo* testing show the inherent advantage of this new, broad spectrum cancer-targeting platform: all APC analogs have identical tumor-specific uptake and persistence regardless of the added radioactive or fluorescence label.[29] Tumor-specific APC uptake partly through the lipid raft-rich compartment of cancer cell membranes, coupled with elimination from normal tissues over time, yields high tumor specific discrimination and targeting for imaging and therapy.[29] Depending on the conjugated radiolabel, CLR1404 may be used for tumor selective PET imaging (^{124}I-CLR1404) or therapeutic radiation (^{131}I-CLR1404). Two fluorescent CLR1404 derivatives were also developed by substituting iodine with fluorescent moieties: CLR1501 (green) and CRL1502 (near infrared) (Figure 1A). CLR1501 and CLR1502 also exhibit tumor selectivity *in vitro* and *in vivo* for human glioblastoma stem-like (GSC) cell lines and xenografts.[29] We envision and are developing the APC cancer-targeting platform for multiple steps in clinical cancer management: diagnostic cancer imaging, surgical tumor detection, and adjuvant cancer therapy. This study compares CLR1501 and CLR1502 with 5-ALA as tumor fluorescence agents, and serves as a proof-of-principle for potential use of fluorescent APC analogs in cancer surgery.

OBJECTIVES

This study aims to 1) define the excitation/emission spectra of CLR1501 and CLR1502, 2) demonstrate CLR1501 and CLR1502 fluorescence differentiates tumor and normal brain in mouse models of orthotopic U251 glioblastoma (GBM) and glioblastoma stem cell (GSC)-derived xenografts, and 3) compare with 5-ALA induced PpIX tumor fluorescence.

METHODS

Fluorescence Spectra Analysis

CLR1501 (18-[p-(4,4-difluoro-4-bora-3a,4a-diaza-s-indacene-8-yl)-phenyl]-octadecyl phosphocholine) and CLR1502 (1,3,3-trimethyl-2-[(E)-2-[(3E)-3-(2-[(2E)-1,3,3-trimethyl-2,3-dihydro-1H-indol-2-ylidene]ethylidene}-2-[4-(18-([2-(trimethylazaniumyl)ethyl phosphonato]oxy)octadecyl)phenyl]cyclohex-1-en-1-yl]ethenyl]-3H-indol-1-ium) were provided by Cellectar Biosciences, Inc. (Madison, WI).[29] Protoporphyrin IX (PpIX) was purchased (P8293, Sigma-Aldrich, St. Louis, MO). CLR1501, CLR1502 and PpIX were diluted in ethanol at 40μg/mL. Ethanol solvent was chosen to avoid unwanted spectral shifts seen with DMSO.[30] The agents were then analyzed in experimental triplicates using the Tecan Safire^2 microplate reader to obtain fluorescence excitation and emission spectra. The following spectra collection parameters were used: 1nm increments, 10nm bandwidth, 10 counts per wavelength, gain of 90. Fluorescence spectra were normalized to peak values.

Orthotopic Glioblastoma Xenograft Model

All studies were performed under approved protocols from the University of Wisconsin-Madison Institutional Review Board and the Animal Care and Use Committee. Non-obese diabetic severe combined immunodeficient (NOD-SCID) mice, U251 glioblastoma line and our patient-derived 22T GBM and GSC lines were used: GSC lines (22CSC, 33CSC, 105CSC) were isolated and validated for multipotent differentiation and tumor initiation via orthotopic xenografts in our lab as previously reported.[31,32] In brief, cells passaged *in vitro* were enzymatically dissociated into single cell suspensions, with between $2x10^5$ to $1x10^6$ cells suspended in 5 μl of phosphate buffered solution (PBS). GSCs were stereotactically injected using a Hamilton syringe into right striatum of anesthetized mice at a rate of 1 μl/min. Coordinates are referenced from bregma: 0 mm antero-posterior, +2.5 mm medio-lateral, and -3.5 mm dorso-ventral.[31-33] At either onset of neurological symptoms, or at 3 months, xenograft formation was verified using T2-weighted magnetic resonance imaging (MRI) using a 4.7T horizontal bore small animal MRI scanner (Varian, Palo Alto, CA).

Fluorescence Agents

CLR1501 and CLR1502 were formulated for intravenous injection as previously described.[29] 5-aminolevulinic acid (5-ALA) purchased commercially (A3785, Sigma-Aldrich, St. Louis, MO) was dissolved in sterile saline. As recommended by the UW Animal Care committee, mice with documented orthotopic GSC or U251 xenografts received ~50-100 μl retro-orbital (RO) injections (equivalent to tail vein injections) [34,35] of CLR1501, CLR1502, 5-ALA, or a combination after isoflurane anesthesia induction: CLR1501 (16 mg/kg, 4 days prior to sacrifice), CLR1502 (2 mg/kg, 4 days prior sacrifice), 5-ALA (100 mg/kg, an average of 5 hours 45 minutes [range 5h10m to 6h13m] prior to sacrifice). After the elapsed time, mice were deeply anesthetized with xylazine/ketamine, then euthanized via perfusion fixation with 4% paraformaldehyde (PFA) in PBS.

Confocal Imaging

Extracted brains were fixed in 4% PFA overnight at 4°C, then placed in 30% sucrose in PBS at 4°C until saturation. Brains were then frozen in Tissue-Tek O.T.C. compound (Sakura Finetek, Torrance, CA) using an isopentane cryobath and stored at -80°C. The brains were cryosectioned at 100 μm, treated with 1 μM ToPro3 iodide nuclear stain in PBS for 15 minutes (T3605 Molecular Probes, Eugene, OR), washed with PBS and mounted with Prolong Gold antifade reagent (P36934 Molecular Probes). Whole brain sections were imaged using a Nikon A1RSi Confocal microscope (Nikon Instruments, Melville, NY) using 10x magnification. CLR1501 fluorescence was imaged using a 488nm excitation laser with a 525/550nm emission filter, and ToPro3 fluorescence was imaged using a 640 nm excitation laser and 650 nm long pass filter. NIS Elements Advanced software was used for measuring average CLR1501 fluorescence intensity of equivalent sized regions of interest (ROI) in tumors versus contralateral brain (determined by ToPro3 nuclear staining).

Ex vivo Flow Cytometry

Tumor xenografts were microscopically dissected from mouse brains with special care to minimize contamination with normal brain parenchyma. Xenografts were enzymatically dissociated using Accutase for 15 mins at 37°C followed by mechanical trituration with P200 pipette. The tissue slurry was filtered with a 40 μm cell strainer and resuspended in flow cytometry buffer (PBS+1% goat serum). Cells were then washed multiple times and analyzed using flow cytometry (FACScalibur, Becton Dickinson). The flow cytometer was corrected for background fluorescence (brain cells from animals that were not injected with CLR1501). Data were collected on 10,000 cells using proper gating for CLR1501 (Ex: 490/Em: 515), and analyzed using WinMDI freeware (http://facs.scripps.edu/software.html). Live cells were gated using forward (FSC) and side (SSC) scatter. Proper gating is established to quantify positive vs. negative fluorescent cells by comparing to isotype controls. Intensity is represented by relative fluorescent units (RFU) or the geometric mean of resulting histograms.

IVIS Spectrum Imaging

PFA perfusion-fixed brains were bisected at the tumor injection site. The IVIS spectrum system (Perkin-Elmer/Xenogen, Waltham, MA) was used to visualize the brains with measurements of average radiance ($p/s/cm^2/sr$) obtained from a standard sized ROI in the tumor comparing with contralateral normal brain, to calculate a ratio of average radiance. The following excitation/emission combinations were used: CLR1501 (500nm/540nm), CLR1502 (745nm/800nm), and 5-ALA (430nm/640nm). After IVIS imaging the brains were embedded in paraffin, sectioned, stained with hematoxylin and eosin (H&E), and imaged with an EVOS XL Core brightfield microscope (Advanced Microscopy Group, Bothell, WA) to verify tumor xenograft. It is important to note that due to technical constraints of the IVIS system, 5-ALA excitation was performed at 430nm (range 415-445nm), and not at the reported optimum of 402nm.

Near infrared (NIR) Imaging

CLR1502 injected mice were imaged with the Fluobeam 800 (Fluoptics, Grenoble, France), which is a hand-held imaging system designed for detecting *in vivo* near infrared fluorescence (excitation laser wavelength of 780 nm and a charge-coupled device (CCD) camera with filters to detect wavelengths > 800nm).[36-38] Imaging was conducted on mice prior to euthanasia and on the exposed or extracted brain after sacrifice. White light photographs were also obtained. The brains were subsequently imaged with the IVIS spectrum system as described above, then embedded in paraffin and processed for general histology. Some brains labeled with CLR1502 were also imaged with a Leica OH4 intraoperative microscope with FL800 attachment (Leica Microsystems, Wetzlar, Germany), designed to image indocyanine green with an 800 nm excitation light and a NIR CCD camera with a 820-860 nm filter.[39,40]

Statistical Analysis

Statistical analyses were done using Microsoft Excel for Mac 2011 Version 14.3.7. Comparisons of mean fluorescence ratio in tumor compared to contralateral normal brain, and T:N ratios between fluorescence agents were performed using a one-tail non-paired Student's T-test. All data with a $p < 0.05$ were considered significant. Numbers of experiments and mice used are indicated.

A total of 35 mice harboring xenografts (25 U251, 10GSC) were imaged on the IVIS system for CLR1501, CLR1502, and/or 5-ALA signal. A total of 9 mice (5 U251, 4 GSC-derived xenografts) were imaged on the Fluobeam near infrared visualization system after CLR1502 injection.

RESULTS

CLR1501 and CLR1502 Spectra

CLR1501 has an excitation peak at 500nm and emission peak at 517nm in the visible green spectrum. CLR1502 has an excitation peak at 760nm and emission peak at 778nm in the near infrared spectrum (Figure 1B). Similar to prior published data, the PpIX fluorescence spectra observed in our lab reveal a 402nm excitation peak and 633 nm emission peak.[10]

Confocal imaging of CLR1501 tumor fluorescence

To avoid ethanol dehydration and extraction of CLR1501 and CLR1502 from tissues, frozen xenograft sections were used for imaging. Confocal imaging of frozen brain sectionsdemonstrated a clear difference in CLR1501 fluorescence between tumor xenografts and contralateral normal brain (figure 1C-E, representative U251 xenograft**)**. For U251 xenografts (n=13) the observed average tumor to contralateral normal brain (T:N) fluorescence ratio was 3.51±0.44 ($p<0.001$). With 22T GBM-derived xenografts, representative magnified views of green fluorescent CLR1501 tumor label show the cellular margin between tumor and normal brain and are shown in Figure 1F-H. For 22CSC xenografts (n=2) the observed T:N fluorescence ratio was 5.84±3.3, though the small sample size limits statistical impact.

CLR1501 tumor fluorescence by flow cytometry

After MRI-verified tumor growth, U251 glioblastoma xenografts from mice injected with CLR1501 (n=4) were removed, analyzed by *ex vivo* flow cytometry, and compared to normal contralateral brain. U251 xenografts revealed a mean T:N ratio of 14.8±7.34 (p=0.07) (Figure 2A).

IVIS tumor fluorescence imaging: CLR1501 versus 5ALA

For all U251 glioblastoma xenografts from mice injected with CLR1501 (n=18) and imaged using IVIS (Ex/Em 500nm/540nm), the mean T:N fluorescence ratio was 7.23±1.63. This was significantly higher than the observed mean T:N ratio of 0.87±0.07 (p<0.001) of the negative controls: U251 xenografts not exposed to CLR1501 (n=7) that were imaged at the same settings.

The observed mean T:N fluorescence ratio was 4.81±0.92 for all U251 xenografts from mice treated with 5-ALA (n=19) and imaged using IVIS (Ex/Em 430/640). This was significantly higher than the observed mean T:N ratio of 1.14±0.19 (p<0.001) of the negative controls, U251 xenografts not treated with 5-ALA (n=6) imaged at the same settings. Overall, CLR1501-treated mice had a higher mean T:N fluorescence ratio than 5-ALA-treated mice, but the difference was not statistically significant (7.23±1.63 versus 4.81±0.92, p = 0.077, NS).

Direct comparison of CLR1501 with 5ALA was performed in 15 mice harboring U251 xenografts that were co-treated with both agents. The observed mean T:N fluorescence ratio was higher for CLR1501 (6.88±1.57) than 5-ALA (4.00±0.97), but the difference was not significant (p=0.066, NS).

The measured average radiance of U251 tumors labeled with CLR1501 ($3.15\times10^8\pm5.66\times10^7$ p/s/cm^2/sr) was higher than tumors labeled with 5-ALA ($2.17\times10^7\pm3.52\times10^6$ p/s/cm^2/sr), but this was in part due to the background auto-fluorescence also higher at the settings used for imaging CLR1501 ($1.67\times10^7\pm3.03\times10^6$ p/s/cm^2/sr) than for 5-ALA imaging settings ($2.93\times10^6\pm4.71\times10^5$ p/s/cm^2/sr).

For 105CSC xenografts the mean T:N fluorescence ratio trended higher for CLR1501 (12.04±3.64, n=2) than for 5-ALA (6.52±1.63, n=3), but this data did not reach significance, partly due to small sample sizes (p=0.17, NS). It is important to note that due to technical constraints of the IVIS system, 5-ALA excitation was performed at 430 nm (range 415-445nm), and not at the reported optimal 402nm wavelength.

IVIS fluorescence imaging: CLR1502 versus 5-ALA and CLR1501

For U251 glioblastoma xenografts in mice treated with CLR1502 (n=5) and imaged using IVIS (Ex/Em 745/800), the mean T:N fluorescence ratio was 9.28±1.08. This is significantly higher than the mean T:N ratio 1.03±0.01 (p<0.001) of negative controls: U251 xenografts in mice not injected with CLR1502 (n=20) imaged at the same settings.

For U251 xenografts the mean T:N ratio was significantly higher for CLR1502 (9.28±1.08) than for 5-ALA (4.81±0.92, p<0.01). Though the mean T:N ratio was higher for CLR1502

(9.28±1.08) than for CLR1501 (7.23±1.63) the difference was not significant (p=0.13, NS) (Figure 2B).

For 33CSC xenografts and 105CSC xenografts the sample size was too small to statistically compare CLR1502 to 5-ALA, but significant CLR1502 tumor fluorescence was observed in xenografts derived from both CSC lines. For 33CSC xenografts the mean T:N ratio for CLR1502 (n=2) was 5.47±3.12. This compares to the 33CSC xenografts mouse (n=1) treated with 5-ALA with a T:N ratio of 6.20. For 105CSC xenografts the mean T:N ratio for CLR1502 (n=3) was 13.31±3.42, which was not statistically significant over the mean T:N ratio for 5-ALA (n=3), which was 6.52±1.63 (p=0.09, NS).

The measured average radiance of U251 tumors labeled with CLR1502 is $6.92\times10^{8}\pm7.30\times10^{7}$ p/s/cm^2/sr, higher than both CLR1501 and 5-ALA labeled tumors, but the background auto-fluorescence measured at the CLR1502 imaging settings is low ($4.45\times10^{6}\pm3.40\times10^{5}$ p/s/cm^2/sr), similar to the auto-fluorescence at the 5-ALA settings, and less than the auto-fluorescence at the CLR1501 settings. As noted above, 5-ALA excitation was performed from 415-445nm, and not at the reported optimal 402nm due to IVIS system technical constraints.

CLR1502 visualization with Fluobeam and the Leica OH4 Microscope

Near-infrared imaging of CLR1502 fluorescence using the Fluobeam device provided excellent macroscopic tumor delineation from normal brain (Figure 3) for all tested GBM/GSC-derived xenografts (U251, 22CSC, 33CSC, 105CSC). Resected tissues with CLR1502 near-infrared fluorescence were confirmed as tumor on H&E sections (Figure 3E) and the adjacent minimally fluorescent tissue confirmed as non-tumor brain (Figure 3F). Under non-optimized conditions, distinct near-infrared tumor fluorescence was also detectable in CLR1502-labeled U251 xenografts (n=2) using a standard Leica OH4 operative microscope with the FL800 attachment (Figure 4). Near-infrared imaging of CLR1502 tumor fluorescence successfully localized tumor through intact skin and skull in a live mouse, and also provided excellent tumor delineation on tumor resection after sacrifice, serving as proof-of-principle for CLR1502 fluorescence-guided tumor surgery (see Video, Supplemental Digital Content, CLR1502 fluorescence visualization of U251-derived xenograft in mouse).

DISCUSSION

Using multiple imaging modalities and primarily the U251 GBM model (and multiple GSC-derived xenografts), this study demonstrated that CLR1501 and CLR1502 provide excellent fluorescence discrimination of tumor from adjacent normal brain. CLR1501 provides fluorescence in the green spectrum (Exc/Em 500nm/517nm) and shows good tumor to brain distinction using confocal microscopy, *ex vivo* flow cytometry, and IVIS spectrum imaging. CLR1502 provides fluorescence in the near-infrared (NIR) spectrum (Exc/Em 760nm/778nm) and shows very high tumor to brain distinction using all three modalities of IVIS spectrum imaging, Fluobeam detection, and commercially available operative microscopes with appropriate fluorescence detection attachments. The capability of already approved and

available commercial imaging systems to visualize these tumor fluorescence agents would accelerate translation to clinical use.

Comparison of CLR1501 and CLR1502 to 5-ALA is important since 5-ALA is the current standard for fluorescence-guided neurosurgery. Using IVIS spectrum imaging of mice harboring U251 GBM xenografts, direct comparison of CLR1501 and CLR1502 to 5-ALA showed that the mean CLR1501 T:N fluorescence ratio is comparable to the 5-ALA ratio, whereas the mean CLR1502 T:N fluorescence ratio was significantly higher than the 5-ALA ratio. Additionally, a near-infrared agent like CLR1502 is attractive for fluorescence-guided resection due to the decreased tissue absorption of light and relative low tissue auto-fluorescence at the near-infrared spectrum. Therefore, use of near-infrared fluorescence will help minimize the loss of signal caused by bleeding during resections.[41,42]

Limitations

Still, a current limitation of using near infrared fluorescence agents in surgery is that tumor is visualized on a separate monitor in a darkened operating theater, and surgeons cannot also simultaneously visualize the resection field and instruments directly as in 5-ALA-guided surgeries under blue light. Conceptual solutions are being developed such as projecting ‘heads-up’ display of the near infrared fluorescence image to one microscope eyepiece, or other methods to enable surgeons to simultaneously see overlapping bright field and near infrared images in the operative microsurgical view. Development of the optimal technologies for practical surgical use of these fluorescent APC analogs is still in progress.

We also acknowledge the inherent limitations in this proof-of-principle study due to using mouse tumor xenograft models derived from implanting human GBM and GSC lines, and non-optimized dosing, administration and detection parameters. Questions relating to optimal APC dose, timing of administration, tumor uptake, persistence of tumor fluorescence, and optimal time window for surgical visualization will need to be answered through clinical trials with human cancer patients. We reported that preclinical and human data obtained with multiple radioiodinated APC analogs with regard to safety, tumor selective uptake and retention were nearly identical likely due to the identical molecular composition of the parental CLR1404 analog [29,43]. Studies with multiple fluorescent (CLR1501, CLR1502) and other APC analogs are underway to directly establish the temporal profile and discover details of their interactions with tumor cells, tumor-brain and blood-brain barriers, especially to determine practical surgical timing, dose, visualization and other parameters.

Clinical Potential

In preparation for clinical trials, the federally mandated safety testing of these novel fluorescent APC analogs was just completed. No overt toxicity was noted with either CLR1501 or CLR1502 during multiple preclinical studies. The parental APC analog CLR1404 (CLR1501 and CLR1502 are fluorescent analogs) has undergone extensive animal and human safety testing. Results from the multi-institutional Phase I trial of therapeutic ^{131}-I-CLR1404 in advanced cancer patients were recently reported.[43]

Radioiodinated APC analogs are currently in Phase 2 clinical trials, and upcoming clinical trials in human tumors are planned for these promising tumor-selective fluorescence agents.

In addition to fluorescence tumor differentiation with CLR1501 and CLR1502, we hypothesize that co-injection with the related radioiodinated ^{124}I-CLR1404 analog (for preoperative PET/CT tumor imaging) would correlate pre-op localization of tumor with intraoperative tumor fluorescence label, and potentially improve extent of resection. Postoperative PET/CT imaging may also provide precise, cellular definition of any residual tumor cells (e.g. define extent of resection).[29] Then, follow-up adjuvant therapies that include administration of therapeutic ^{131}I-CLR1404 would target residual or unresectable tumor cells remaining after maximal surgery.[29] Clinical trials to optimize imaging dose and timing parameters are underway for the radioiodinated APC analogs, and will prove useful for optimizing fluorescent APC surgical clinical trials to achieve the multi-modality strategy of using APC diagnostics and therapeutics against cancer.

CONCLUSION

CLR1501 (green, Exc/Em 500nm/517nm) and CLR1502 (near-infrared, Exc/Em 760nm/778nm) are novel fluorescent derivatives of tumor-targeting alkylphosphocholine analogs.[29] Their tumor fluorescence is readily detected with current clinically used, readily available indocyanine green fluorescence microscopes, and may not require new equipment purchases. CLR1501 and CLR1502 provided excellent tumor to normal brain fluorescence discrimination with *in vivo* glioblastoma (GBM) and glioblastoma stem cell (GSC)-derived xenograft mouse models. In comparison with 5-ALA, CLR1502 showed a superior tumor to brain fluorescence ratio. This study demonstrates the practical and promising potential of CLR1501 and CLR1502 analogs for use in fluorescence-guided tumor surgery.

Supplementary Material

Refer to Web version on PubMed Central for supplementary material.

Acknowledgements

We thank Anatoly Pinchuk for APC analog synthesis and analysis, and Marc Longino for formulating agents for in vivo injection. These NIH grants provided partial support: R21CA161704 (P.A.C, J.S.K.), MSTP training fellowship (UW MSTP T32GM008692 to R.R.Z.), R01CA158800 (J.S.K, J.P.W.), R01NS075995 (J.S.K.). We appreciate unrestricted support from the Headrush Brain Tumor Research Professorship and Roger Loff Memorial Fund for GBM Research (J.S.K.). General funding were provided by UW Carbone Cancer Center, Wisconsin Partnership Program core grant support of the Center for Stem Cell and Regenerative Medicine, from the University of Wisconsin (Graduate School, Depts. of Radiology, Medical Physics, Human Oncology, Neurological Surgery, Wisconsin Alumni Research Foundation, and Wisconsin Institutes of Discovery). Pilot grants and small animal imaging were supported by the UW Carbone Cancer Center National Cancer Institute Support grant (P30 CA014520), Waisman Center core grant from the National Institute of Child Health and Human Development (P30 HD03352).

REFERENCES

1. Lacroix M, Abi-Said D, Fourney DR, et al. A multivariate analysis of 416 patients with glioblastoma multiforme: prognosis, extent of resection, and survival. J Neurosurg. Aug; 2001 95(2):190–198. [PubMed: 11780887]

2. McGirt MJ, Chaichana KL, Gathinji M, et al. Independent association of extent of resection with survival in patients with malignant brain astrocytoma. J Neurosurg. Jan; 2009 110(1):156–162. [PubMed: 18847342]

3. Sanai N, Snyder LA, Honea NJ, et al. Intraoperative confocal microscopy in the visualization of 5-aminolevulinic acid fluorescence in low-grade gliomas. J Neurosurg. Oct; 2011 115(4):740–748. [PubMed: 21761971]

4. Sanai N, Polley MY, McDermott MW, Parsa AT, Berger MS. An extent of resection threshold for newly diagnosed glioblastomas. J Neurosurg. Jul; 2011 115(1):3–8. [PubMed: 21417701]

5. Liu JT, Meza D, Sanai N. Trends in fluorescence image-guided surgery for gliomas. Neurosurgery. Jul; 2014 75(1):61–71. [PubMed: 24618801]

6. Kubben PL, ter Meulen KJ, Schijns OE, ter Laak-Poort MP, van Overbeeke JJ, van Santbrink H. Intraoperative MRI-guided resection of glioblastoma multiforme: a systematic review. Lancet Oncol. Oct; 2011 12(11):1062–1070. [PubMed: 21868286]

7. Inoue K, Fukuhara H, Shimamoto T, et al. Comparison between intravesical and oral administration of 5-aminolevulinic acid in the clinical benefit of photodynamic diagnosis for nonmuscle invasive bladder cancer. Cancer. Feb 15; 2012 118(4):1062–1074. [PubMed: 21773973]

8. van Dam GM, Themelis G, Crane LM, et al. Intraoperative tumor-specific fluorescence imaging in ovarian cancer by folate receptor-alpha targeting: first in-human results. Nat Med. Oct; 2011 17(10):1315–1319. [PubMed: 21926976]

9. Stummer W, Stocker S, Wagner S, et al. Intraoperative detection of malignant gliomas by 5-aminolevulinic acid-induced porphyrin fluorescence. Neurosurgery. Mar; 1998 42(3):518–525. discussion 525-516. [PubMed: 9526986]

10. Shepherd M, Dailey HA. A continuous fluorimetric assay for protoporphyrinogen oxidase by monitoring porphyrin accumulation. Anal Biochem. Sep 1; 2005 344(1):115–121. [PubMed: 16039600]

11. Stummer W, Novotny A, Stepp H, Goetz C, Bise K, Reulen HJ. Fluorescence-guided resection of glioblastoma multiforme by using 5-aminolevulinic acid-induced porphyrins: a prospective study in 52 consecutive patients. J Neurosurg. Dec; 2000 93(6):1003–1013. [PubMed: 11117842]

12. Stummer W, Stepp H, Moller G, Ehrhardt A, Leonhard M, Reulen HJ. Technical principles for protoporphyrin-IX-fluorescence guided microsurgical resection of malignant glioma tissue. Acta Neurochir (Wien). 1998; 140(10):995–1000. [PubMed: 9856241]

13. Stummer W, Stocker S, Novotny A, et al. In vitro and in vivo porphyrin accumulation by C6 glioma cells after exposure to 5-aminolevulinic acid. J Photochem Photobiol B. Sep; 1998 45(2-3): 160–169. [PubMed: 9868806]

14. Stummer W, Pichlmeier U, Meinel T, et al. Fluorescence-guided surgery with 5-aminolevulinic acid for resection of malignant glioma: a randomised controlled multicentre phase III trial. Lancet Oncol. May; 2006 7(5):392–401. [PubMed: 16648043]

15. Diez Valle R, Tejada Solis S, Idoate Gastearena MA, Garcia de Eulate R, Dominguez Echavarri P, Aristu Mendiroz J. Surgery guided by 5-aminolevulinic fluorescence in glioblastoma: volumetric analysis of extent of resection in single-center experience. J Neurooncol. Mar; 2011 102(1):105–113. [PubMed: 20607351]

16. Hefti M, von Campe G, Moschopulos M, Siegner A, Looser H, Landolt H. 5-aminolevulinic acid induced protoporphyrin IX fluorescence in high-grade glioma surgery: a one-year experience at a single institutuion. Swiss Med Wkly. Mar 22; 2008 138(11-12):180–185. [PubMed: 18363116]

17. Roberts DW, Valdes PA, Harris BT, et al. Coregistered fluorescence-enhanced tumor resection of malignant glioma: relationships between delta-aminolevulinic acid-induced protoporphyrin IX fluorescence, magnetic resonance imaging enhancement, and neuropathological parameters. Clinical article. J Neurosurg. Mar; 2011 114(3):595–603. [PubMed: 20380535]

18. Panciani PP, Fontanella M, Schatlo B, et al. Fluorescence and image guided resection in high grade glioma. Clin Neurol Neurosurg. Jan; 2012 114(1):37–41. [PubMed: 21963142]

19. Nabavi A, Thurm H, Zountsas B, et al. Five-aminolevulinic acid for fluorescence-guided resection of recurrent malignant gliomas: a phase ii study. Neurosurgery. Dec; 2009 65(6):1070–1076. discussion 1076-1077. [PubMed: 19934966]

20. Eschbacher J, Martirosyan NL, Nakaji P, et al. In vivo intraoperative confocal microscopy for real-time histopathological imaging of brain tumors. J Neurosurg. Apr; 2012 116(4):854–860. [PubMed: 22283191]
21. Nikolay M, Cavalcanti D, Eschbacher J, et al. Use of Indocyanine Green Near-Infrared Laser Confocal Endomicroscopy In Vivo: Potential to Intraoperatively Detect the Boundary of Infiltrative Tumor. Neurosurgery. 2011
22. Sanai, N.; Eschbacher, J.; Hattendorf, G., et al. Neurosurgery. Vol. 68. 2 Suppl Operative: Jun. 2011 Intraoperative confocal microscopy for brain tumors: a feasibility analysis in humans.; p. 282-290.discussion 290
23. Sankar T, Delaney PM, Ryan RW, et al. Miniaturized handheld confocal microscopy for neurosurgery: results in an experimental glioblastoma model. Neurosurgery. Feb; 2010 66(2):410–417. discussion 417-418. [PubMed: 20087141]
24. Schlosser HG, Suess O, Vajkoczy P, van Landeghem FK, Zeitz M, Bojarski C. Confocal neurolasermicroscopy in human brain - perspectives for neurosurgery on a cellular level (including additional comments to this article). Cent Eur Neurosurg. Feb; 2010 71(1):13–19. [PubMed: 19787571]
25. Kim A, Khurana M, Moriyama Y, Wilson BC. Quantification of in vivo fluorescence decoupled from the effects of tissue optical properties using fiber-optic spectroscopy measurements. J Biomed Opt. Nov-Dec;2010 15(6):067006. [PubMed: 21198210]
26. Valdes PA, Kim A, Brantsch M, et al. delta-aminolevulinic acid-induced protoporphyrin IX concentration correlates with histopathologic markers of malignancy in human gliomas: the need for quantitative fluorescence-guided resection to identify regions of increasing malignancy. Neuro Oncol. Aug; 2011 13(8):846–856. [PubMed: 21798847]
27. Valdes PA, Leblond F, Jacobs VL, Wilson BC, Paulsen KD, Roberts DW. Quantitative, spectrally-resolved intraoperative fluorescence imaging. Sci Rep. Nov 12.2012 2:798. [PubMed: 23152935]
28. Valdes PA, Leblond F, Kim A, et al. Quantitative fluorescence in intracranial tumor: implications for ALA-induced PpIX as an intraoperative biomarker. J Neurosurg. Jul; 2011 115(1):11–17. [PubMed: 21438658]
29. Weichert JP, Clark PA, Kandela IK, et al. Alkylphosphocholine analogs for broad-spectrum cancer imaging and therapy. Sci Transl Med. Jun 11.2014 6(240):240ra275.
30. Pretsch, E.; Bühlmann, P.; Badertscher, M. Solvent Corrections. Springer; Berlin: 2009. p. 401-420.
31. Clark PA, Iida M, Treisman DM, et al. Activation of multiple ERBB family receptors mediates glioblastoma cancer stem-like cell resistance to EGFR-targeted inhibition. Neoplasia. May; 2012 14(5):420–428. [PubMed: 22745588]
32. Zorniak M, Clark PA, Leeper HE, et al. Differential expression of 2′,3′-cyclic-nucleotide 3′-phosphodiesterase and neural lineage markers correlate with glioblastoma xenograft infiltration and patient survival. Clin Cancer Res. Jul 1; 2012 18(13):3628–3636. [PubMed: 22589395]
33. Galli R, Binda E, Orfanelli U, et al. Isolation and characterization of tumorigenic, stem-like neural precursors from human glioblastoma. Cancer Res. Oct 1; 2004 64(19):7011–7021. [PubMed: 15466194]
34. Nanni C, Pettinato C, Ambrosini V, et al. Retro-orbital injection is an effective route for radiopharmaceutical administration in mice during small-animal PET studies. Nucl Med Commun. Jul; 2007 28(7):547–553. [PubMed: 17538396]
35. Yardeni T, Eckhaus M, Morris HD, Huizing M, Hoogstraten-Miller S. Retro-orbital injections in mice. Lab Anim (NY). May; 2011 40(5):155–160. [PubMed: 21508954]
36. Keramidas M, Josserand V, Righini CA, Wenk C, Faure C, Coll JL. Intraoperative near-infrared image-guided surgery for peritoneal carcinomatosis in a preclinical experimental model. Br J Surg. May; 2010 97(5):737–743. [PubMed: 20309948]
37. Mery E, Jouve E, Guillermet S, et al. Intraoperative fluorescence imaging of peritoneal dissemination of ovarian carcinomas. A preclinical study. Gynecol Oncol. Jul; 2011 122(1):155–162. [PubMed: 21463889]

38. Wenk CH, Ponce F, Guillermet S, et al. Near-infrared optical guided surgery of highly infiltrative fibrosarcomas in cats using an anti-alphavss3 integrin molecular probe. Cancer Lett. Jul 1; 2013 334(2):188–195. [PubMed: 23200675]

39. Gioux S, Choi HS, Frangioni JV. Image-guided surgery using invisible near-infrared light: fundamentals of clinical translation. Mol Imaging. Oct; 2010 9(5):237–255. [PubMed: 20868625]

40. Raabe A, Nakaji P, Beck J, et al. Prospective evaluation of surgical microscope-integrated intraoperative near-infrared indocyanine green videoangiography during aneurysm surgery. J Neurosurg. Dec; 2005 103(6):982–989. [PubMed: 16381184]

41. Frangioni JV. In vivo near-infrared fluorescence imaging. Curr Opin Chem Biol. Oct; 2003 7(5): 626–634. [PubMed: 14580568]

42. Gibbs SL. Near infrared fluorescence for image-guided surgery. Quant Imaging Med Surg. Sep; 2012 2(3):177–187. [PubMed: 23256079]

43. Grudzinski J, Titz B, Kozak K, et al. A Phase 1 Study of 131I-CLR1404 in Patients with Relapsed or Refractory Advanced Solid Tumors: Dosimetry, Biodistribution, Pharmacokinetics, and Safety. PLoS one. (in press).

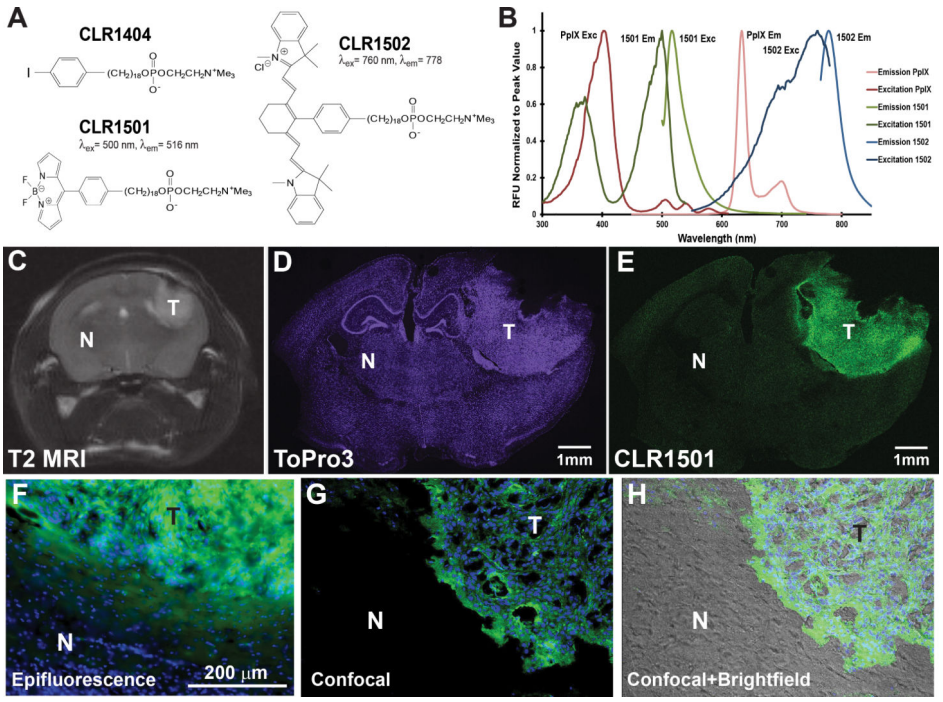

Figure 1.

(A) Chemical structures of APC analogs. (B) Fluorescence spectra: CLR1501 (excitation peak 500nm, emission peak 517nm). CLR1502 (excitation peak 760nm, emission peak 778nm). PpIX (excitation peak 402nm, emission peak 633nm). (C-E) U251-derived orthotopic brain tumor verified by MRI (C, T2-weighted) and labeled with CLR1501 (E), with ToPro3 nuclear counterstain (D). (F-H) Histological analysis of brain-tumor interface in 22T GBM-derived orthotopic xenograft labeled with CLR1501 (green) (F) epifluorescence visualization of xenograft-brain border with blue DAPI nuclear counterstain. (G) Confocal view of xenograft labeled with CLR1501. (H) Confocal and brightfield view of xenograft and adjacent normal brain. T: tumor, N: normal brain.

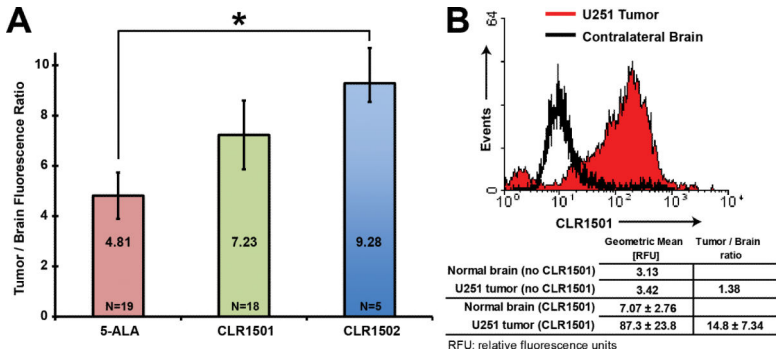

Figure 2.

(A) CLR1501 tumor to brain fluorescence ratios for U251-derived orthotopic xenograft. (B) Flow cytometry of CLR1501^{+} cells from U251-derived orthotopic xenograft compared to normal brain.

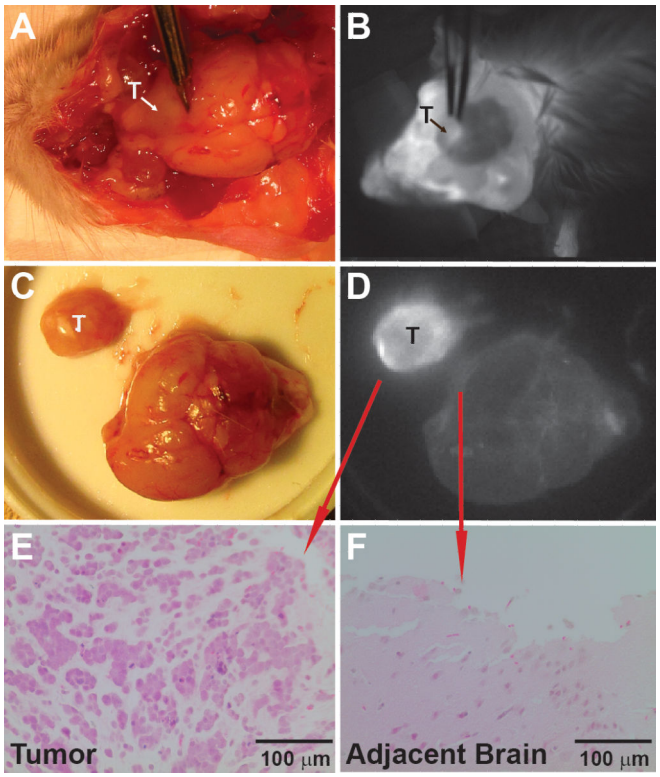

Figure 3.

(A, B) CLR1502 fluorescence of 22 GSC-derived orthotopic xenograft (B) compared to visible light (A). (C, D) CLR1502 fluorescence of 22 GSC-derived xenograft demonstrating excellent macroscopic tumor delineation from normal brain (D), compared to visible light (C). (E, F) Verification of tumor (E) and normal brain (F) by histology (H&E). T: tumor, N: normal brain.

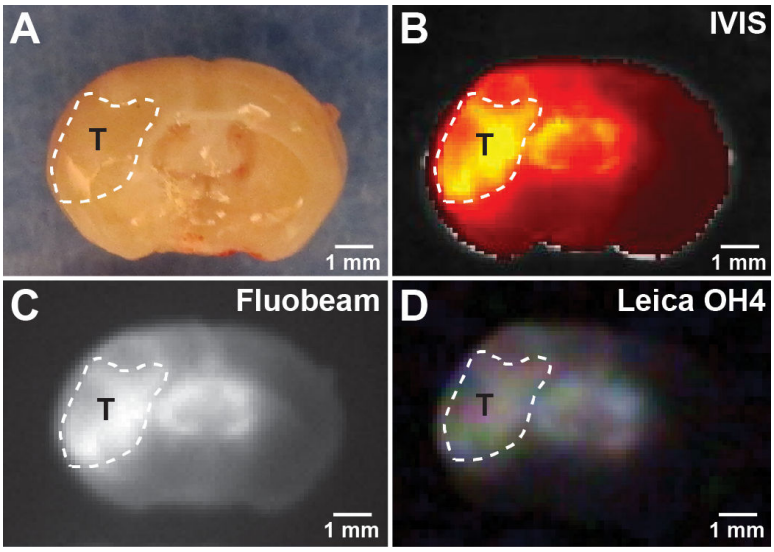

Figure 4.

Comparison of non-optimized CLR1502 tumor fluorescent visualization using visible light (A), preclinical IVIS-Spectrum (B) and Fluobeam (C), and clinical Leica OH4 (D) systems. T: tumor xenograft, outlined by dotted line.